The Journal of Neuroscience, April 1993, 13(4): 1429–1440

Assembly of $GABA_A$ Receptor Subunits: $\alpha_1\beta_1$ and $\alpha_1\beta_1\gamma_{2S}$ Subunits Produce Unique Ion Channels with Dissimilar Single-Channel Properties

Timothy P. Angelotti[1] and Robert L. Macdonald[2,3]

Departments of [1]Pharmacology, [2]Neurology, and [3]Physiology, University of Michigan Medical School, Ann Arbor, Michigan 48109-1687

Recent experimental evidence has led to the hypothesis that $GABA_A$ receptor channel (GABAR) heterogeneity or receptor channel subtypes may occur by differential assembly of a given set of subunits into various configurations. Alternatively, assembly of subunits into mature GABARs may arise from an ordered process to produce a preferred form of the receptor channel, as seen for nicotinic ACh receptors. In the preceding article, we demonstrated that transient expression of GABAR α_1 and β_1 subunits in mouse L929 fibroblast cells produced two different types of GABARs, when coexpressed with and without the γ_{2S} subunit. Not only did these GABARs differ in their GABA and diazepam pharmacology, but initial single-channel recordings suggested that the two types of GABARs ($\alpha_1\beta_1$ and $\alpha_1\beta_1\gamma_{2S}$) had different conductance and gating properties. It also appeared that $\alpha_1\beta_1\gamma_{2S}$ GABARs were preferentially formed over $\alpha_1\beta_1$ GABARs, but it was not completely shown if both forms of GABARs were produced when a cell expressed all three subunits. To characterize further the assembly process and determine the preferred form, if it existed, it was necessary to obtain a kinetic "fingerprint" for both $\alpha_1\beta_1$ and $\alpha_1\beta_1\gamma_{2S}$ GABARs. Thus, single-channel patch-clamp recording and kinetic analysis of receptor channel gating were performed. For both $\alpha_1\beta_1$ and $\alpha_1\beta_1\gamma_{2S}$ GABARs, GABA evoked single-channel openings to both a main conductance (15 and 29 pS, respectively) and a subconductance level (10 and 21 pS, respectively) with greater than 90% of the total current through the main conductance level openings. The two GABAR populations were further differentiated by their open and burst properties. On average, $\alpha_1\beta_1\gamma_{2S}$ GABARs opened for almost three times the duration as $\alpha_1\beta_1$ GABARs (6.0 vs 2.3 msec, respectively) and had three openings per burst. $\alpha_1\beta_1$ GABARs opened predominantly as single opening bursts. Using the conductance and gating properties to differentiate the two GABAR populations, we determined that $\alpha_1\beta_1$ GABARs were rarely, if ever, formed upon coexpression of all three subunits, suggesting that $\alpha_1\beta_1\gamma_{2S}$ GABARs were the preferred final form of the receptor channel. Also, the homogeneity of the conductance and gating properties of $\alpha_1\beta_1\gamma_{2S}$ GABARs among the different patches studied implied that a single preferred configuration of GABARs may exist. Thus, the assembly of GABARs from their constituent subunits may occur by an ordered, not random, process akin to nicotinic ACh receptors, suggesting another conserved feature of members of the ligand-gated ion channel supergene family.

[Key words: assembly, conductance, gating properties, patch clamp, recombinant DNA, transient expression]

Since the initial cloning of multiple $GABA_A$ receptor subunits (for a review, see Olsen and Tobin, 1990), it has been demonstrated that functional GABA receptor channels (GABARs) could be assembled from single-, double-, and triple-subunit combinations, depending upon the cell type used for expression (Schofield et al., 1987; Blair et al., 1988; Shivers et al., 1989; Sigel et al., 1990). Assuming a random pentameric arrangement of receptor subunits to form the ion channel pore, Burt and Kamatchi (1991) calculated that one, two, or three receptor subunits expressed in a cell could assemble into one, eight, and fifty-one different configurations, respectively. It is not known whether all of these different pentameric arrangements actually assemble, produce functional receptors, and possess different pharmacological or biophysical properties, or if instead a single configuration exists as the preferred form. In comparison, the muscle nicotinic ACh receptor, which is composed of α, β, γ, or ϵ, and δ subunits and could randomly assemble into 208 different pentameric configurations, prefers to form a single pentameric structure, $\alpha_2\beta\gamma\delta$ or $\alpha_2\beta\epsilon\delta$ (Toyoshima and Unwin, 1990). In fact, it has been shown that the assembly of nicotinic ACh receptors proceeds along an ordered pathway starting with the formation of $\alpha\gamma$ and $\alpha\delta$ dimers, eventually proceeding to form the mature receptor (Blount et al., 1990; Paulson et al., 1991; Saedi et al., 1991). Receptors with less than all four nicotinic subunits can assemble into functional ion channels, albeit at a lower efficiency and with different biophysical properties than the preferred form of the receptor (Kullberg et al., 1990; Sumikawa and Gehle, 1992). It remains to be determined if the assembly of GABARs proceeds along a random pathway as suggested by some expression studies or if there exists a preferred final form(s) of the receptor.

Heterologous expression of various GABAR subunits has been utilized to determine the specific pharmacological and biophysical properties of receptors formed by different subunits (Levitan et al., 1988; Sigel et al., 1990; Verdoorn et al., 1990; Smart et al., 1991; Knoflach et al., 1992). Whole-cell currents

Received June 18, 1992; revised Sept. 2, 1992; accepted Sept. 16, 1992.

This work was supported by a grant from the Lucille P. Markey Charitable Trust Fund and U.S. Public Health Service grant P01 NS19163 to R.L.M. T.P.A. is a recipient of a PMA Foundation predoctoral fellowship and National Institutes of Health Training Grant GM 07767-14. This work has been presented by T.P.A. in partial fulfillment of the requirements for the degree of Doctorate of Philosophy in Pharmacology from the University of Michigan.

Correspondence should be addressed to Robert L. Macdonald, M.D., Ph.D., Department of Neurology, 1103 East Huron Street, University of Michigan, Medical School, Ann Arbor, MI 48109-1687.

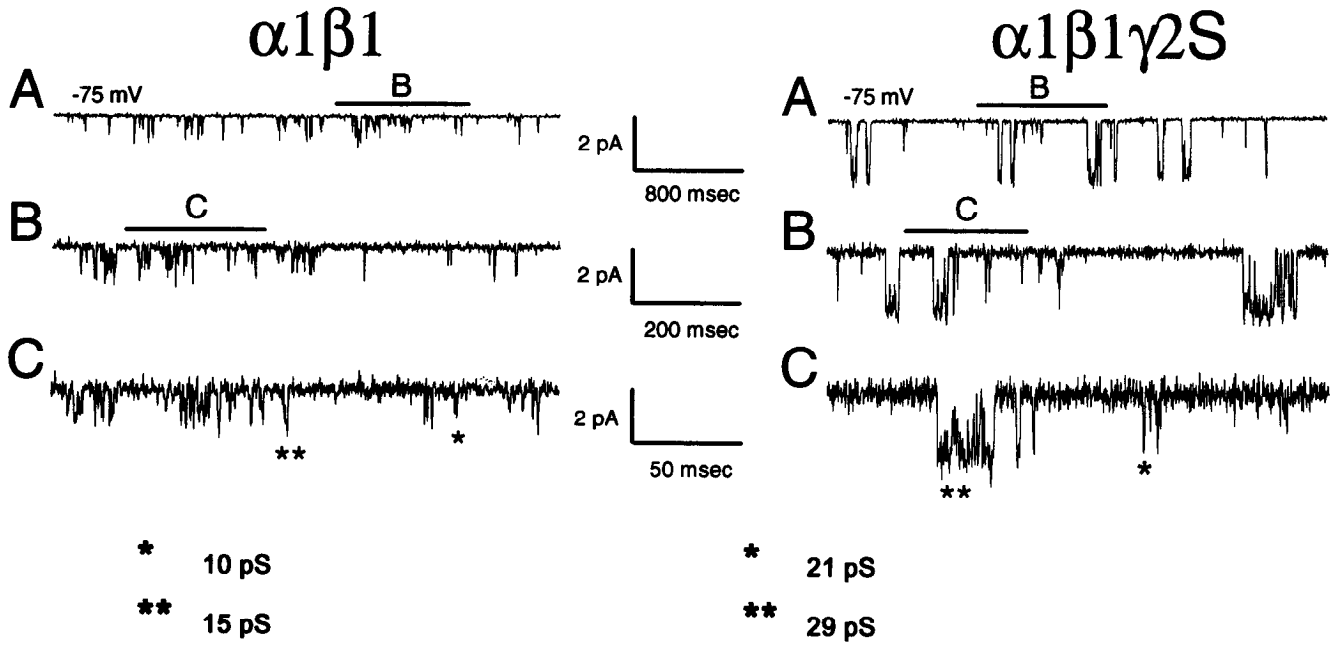

Figure 1. $\alpha_1\beta_1$ and $\alpha_1\beta_1\gamma_{2S}$ GABAR single-channel currents. Representative single-channel openings evoked by 3 μM GABA (applied for the duration of the trace) were recorded from outside-out patches excised from L929 cells after transfection with either α_1 and β_1 (*left*) or α_1, β_1, and γ_{2S} subunit cDNAs (*right*). Recombinant receptor-expressing cells were identified by FDG staining before study. Records *B* and *C* are higher-resolution tracings of *A*, as delineated by the *labeled bars*. The holding potential was −75 mV. Representative openings to the $\alpha_1\beta_1$ and $\alpha_1\beta_1\gamma_{2S}$ GABAR subconductance (10 and 21 pS, respectively) and main conductance levels (15 and 29 pS respectively) are denoted by *asterisks* (*, subconductance; **, main conductance level). Note the difference in amplitude and temporal properties of the $\alpha_1\beta_1$ and $\alpha_1\beta_1\gamma_{2S}$ subunit combinations.

from cells expressing three subunits represent the summation of single-channel currents produced by all potential single-, double-, and triple-subunit combinations and possibly different subunit configurations. The low resolution of such experiments did not permit a characterization of functional receptor heterogeneity, if it existed. An exception to this was the demonstration that Zn^{2+}-sensitive $\alpha_1\beta_2$ GABARs were rarely formed when α_1, β_2, and γ_{2S} subunits were coexpresed to produce a Zn^{2+}-insensitive $\alpha_1\beta_2\gamma_{2S}$ GABAR (Draguhn et al., 1990). It is still possible that distinct GABARs that were all insensitive to Zn^{2+} inhibition were formed, but they could not be resolved using the voltage-clamp recording technique applied to whole cells.

Single-channel recording techniques may overcome the limitations of the whole-cell recording technique, since GABARs formed by different subunit combinations may have unique single-channel properties. It has been demonstrated (Moss et al., 1990; Verdoorn et al., 1990), that $\alpha\beta$, $\alpha\gamma$, and $\alpha\beta\gamma$ subunit combinations can produce GABARs with different single-channel conductances, but their gating properties have not been established. It is possible that some of the potential arrangements of GABAR subunits could give rise to ion channels with unique single-channel properties even when data obtained using voltage-clamp or whole-cell recording techniques were inconclusive. By comparing the single-channel properties of GABARs produced with coexpression of two or more subunits in a cell, it may be possible to determine how many variant configurations of the receptor can be assembled and if there is a preferred final form.

In the preceding study, using a marker gene/fluorescent substrate technique (Angelotti et al., 1993), we transfected mouse L929 fibroblast cells with various double- and triple-subunit combinations of α_1, β_1, and γ_{2S} subunits cDNAs. Unexpectedly, expression of $\alpha_1\beta_1$ and $\alpha_1\beta_1\gamma_{2S}$ GABARs, but not $\alpha_1\gamma_{2S}$ and $\beta_1\gamma_{2S}$ GABARs, occurred in positively transfected cells. Expression of GABARs consisting of either $\alpha_1\beta_1$ or $\alpha_1\beta_1\gamma_{2S}$ subunits produced different whole-cell current properties (Angelotti et al., 1993). GABAR whole-cell currents from individual cells expressing $\alpha_1\beta_1$ subunits had a much shallower GABA concentration–response curve and smaller peak amplitude currents. The fourfold difference in the magnitude of the whole-cell $\alpha_1\beta_1$ and $\alpha_1\beta_1\gamma_{2S}$ GABAR currents recorded could have been due to a difference in the number of GABARs expressed per cell, with each type having similar single-channel properties. Alternatively, there may be differences in certain single-channel parameters between the two receptor populations, including a difference in conductance levels, current–voltage relationships, gating properties, or a combination of all three attributes. Also, it was possible that the currents arising from cells transfected with $\alpha_1\beta_1\gamma_{2S}$ subunit cDNAs were made of a combination of $\alpha_1\beta_1$ GABARs and a unique receptor(s) containing all three subunits. Raw data tracings of single-channel openings from L929 cells expressing either $\alpha_1\beta_1$ or $\alpha_1\beta_1\gamma_{2S}$ subunits suggested that each opened to different current levels, with the $\alpha_1\beta_1$ GABAR currents being smaller in amplitude than the $\alpha_1\beta_1\gamma_{2S}$ GABAR currents (Angelotti et al., 1993). To examine further the process of GABAR assembly, these experiments were extended by using the techniques of single-channel patch-clamp recording and kinetic analysis of GABAR gating.

Materials and Methods

Sources. FDG and Imagene were purchased from Molecular Probes, Inc. (Eugene, OR). All other chemicals, drugs, sera, media, and cell attachment factors were obtained from GIBCO–Bethesda Research Labs (BRL) (Bethesda, MD), Boehringer Mannheim Biochemicals (India-

napolis, IN), or Sigma Chemicals (St. Louis, MO). Tissue culture dishes were purchased from Corning Glass Works (Corning, NY). All cell lines were purchased from American Type Culture Collection (Rockford, MD). Restriction and DNA modification enzymes were obtained from either BRL, Boehringer Mannheim Biochemicals, or New England Biolabs, Inc. (Beverly, MA). Diazepam was kindly provided by Hoffmann–LaRoche (Nutley, NJ). Gridded 35 mm plates were produced using a Mecanex BB Form 2 according to the manufacturer's instructions (Medical Systems, Inc., Greenvale, NY). Gridded plates were retreated with a corona discharge by Corning, Inc.

Plasmid construction. The expression vectors encoding the bovine α_1 and β_1 and human γ_{2S} subunits of the GABAR and *Escherichia coli* β-galactosidase gene (*lacZ*) used in these experiments have been described previously (pCMVbα_1, pCMVbβ_1, pCMVhγ_{2S}, and pCMVβGal, respectively) (Angelotti et al., 1993).

Cell culture and DNA transfection. Mouse L929 cells were grown in Dulbecco's modified Eagle's medium with 10% horse serum with 100 IU/ml penicillin and 100 μg/ml streptomycin, at 37°C in 5% CO_2, 95% air. For transfections, cell lines were passaged and plated as described previously (Angelotti et al., 1993). Cells were transfected using the modified calcium phosphate precipitation method (Chen and Okayama, 1987) with various combinations of CsCl-banded expression vectors in either a 1:1:1:1 ratio (α_1:β_1:γ_{2S}:*lacZ*) or in a 1:1:1 ratio (α_1:β_1:*lacZ*). The total amount of DNA added per 60 mm dish was 9.6 μg in 300 μl of transfection buffer. Transfected cells were shocked with glycerol solution, replated onto gridded plates, and prepared for electrophysiological recording as described previously (Angelotti et al., 1993). GABARs expressed after transfection with more than one GABAR cDNA could express multiple types of GABARs.

β-Galactosidase staining protocols. 5-Bromo-4-chloro-3-indoyl β-D-galactoside (X-Gal) and fluorescein-di-β-galactopyranoside (FDG) staining was performed as described previously (Angelotti et al., 1993).

Electrophysiological analysis. Prior to recording, the PBS/FDG solution on the plate of cells was exchanged with multiple washings of external recording medium containing the following (in mM): 142 NaCl, 8.1 KCl, 6 $MgCl_2$, 10 mM glucose, 10 HEPES (pH 7.4). The intrapipette solution contained (in mM): 153 KCl, 1 $MgCl_2$, 5 mM EGTA, and 10 mM HEPES (pH 7.3). This combination of external and intrapipette solutions produced a chloride equilibrium potential (E_{Cl}) of approximately 0 mV and a potassium equilibrium potential (E_K) of -75 mV across the patch membrane. A GABA stock solution (10 mM) was diluted with external recording solution to the indicated final concentration on the day of the experiment. Drugs were applied by a pressure ejection micropipette (10–15 μm tip diameter, 0.5–1.0 psi) placed next to the cell or patch. Single-channel current recording was performed with methods described previously for mouse spinal cord neuron recordings (Macdonald et al., 1989; Porter et al., 1990) using a List L/M EPC-7 amplifier (Darmstadt, Germany). Data from two or more separate transfections were pooled for analysis. The results did not vary between transections. All recordings were done at room temperature (22–24°C).

Single-channel data collection and analysis. Currents were recorded simultaneously on a video cassette recorder (Sony SL-2700, modified to 0–20 kHz) via a digital audio processor (PCM-2, Medical Systems Corp., Greenvale, NY) and a chart recorder (Gould Inc., Cleveland, OH) for later computer analysis. Whole-cell and single-channel recordings were low-passed filtered (3 dB at 1 kHz, eight-pole Bessel filter, Frequency Devices) before the chart recorder. Single-channel currents were low-pass filtered (3 dB at 10 kHz, eight-pole Bessel filter) before recording on video cassette tape.

For single-channel analysis, the data were replayed from the video cassette recorder tape and digitized (20 kHz sampling rate, 14 bit/0.024 pA resolution, 2 kHz low-pass eight-pole Bessel filter interposed). Current durations were determined using computer software developed in this laboratory. The software and open, burst, and closed duration criteria are described elsewhere (Macdonald et al., 1989). Valid openings and closings were detected using the 50% threshold crossing method and were accepted as valid events if their durations were greater than twice the measured system rise time (rise time, 130 μsec). Bursts were defined as openings or groups of openings separated by relatively long closed periods (t_c) (Colquhoun and Sigworth, 1983), which was set at 5 msec (Macdonald et al., 1989).

Open, burst, and closed durations were placed into either linear or logarithmic bins and plotted in appropriate frequency histograms to minimize bin promotion errors (McManus et al., 1987). For linear open

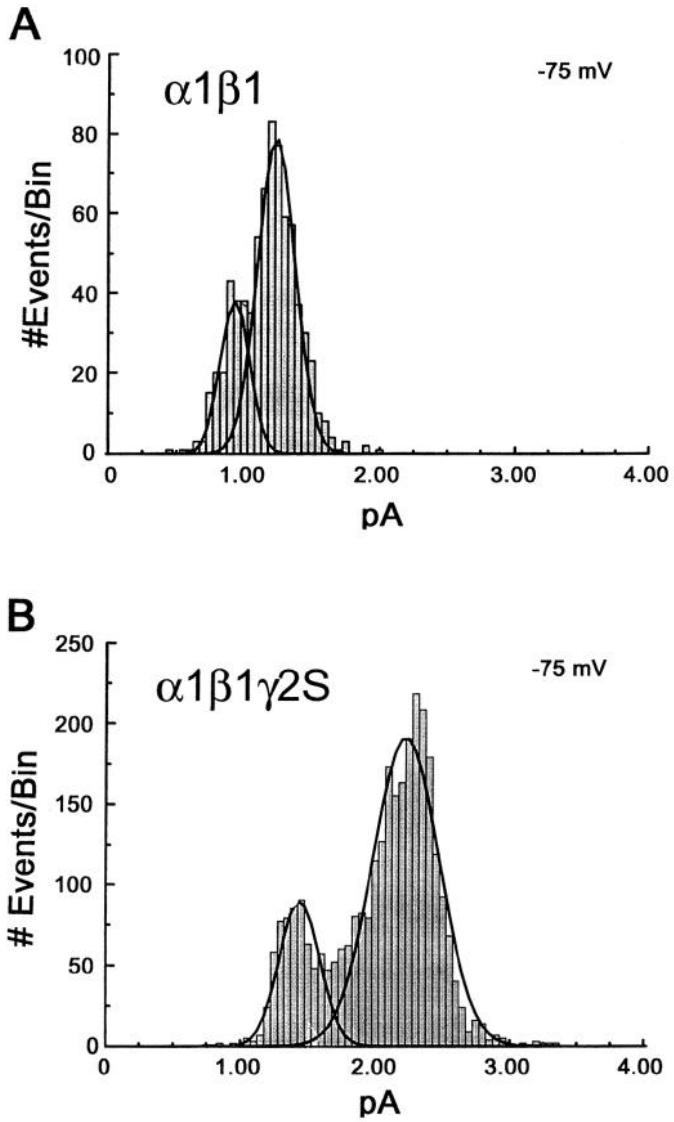

Figure 2. Amplitudes of $\alpha_1\beta_1$ and $\alpha_1\beta_1\gamma_{2S}$ GABAR single-channel openings. Amplitude histograms of GABA-evoked openings (1–10 μM, -75 mV) from excised outside-out patches from transfected cells (*A*, $\alpha_1\beta_1$; *B*, $\alpha_1\beta_1\gamma_{2S}$) were constructed as described (see Materials and Methods). For each receptor combination, the histogram was fitted best by the sum of two Gaussian curves representing a main and a subconductance level. For the $\alpha_1\beta_1$ subunit combination shown above, the mean values were 0.90 and 1.24 pA, and for the $\alpha_1\beta_1\gamma_{2S}$ subunit combination, 1.46 and 2.24 pA (subconductance and main conductance level, respectively).

and burst duration histograms, durations were binned into 0.5 msec bins. For closed duration histograms, logarithmic binning using a logarithmic time axis and a square-root ordinate transformation was used (Sigworth and Sine, 1987). The closed durations were binned using 42 bins and 10 bins/decade resolution with a 300 μsec lower limit. Nonlinear curve fitting was performed using the method of maximum likelihood of fit for all frequency histograms (Colquhoun and Sigworth, 1983). Error ranges of components were determined by likelihood intervals ($m = 2$ to approximate 95% confidence intervals), and the number of significant exponential components was determined as described previously (Macdonald et al., 1989).

The presence of undetected openings, bursts, and closings can cause measured open, burst, and closed durations to be longer than "true" open, burst, and closed durations. Throughout the text, open, burst, and closed durations will refer to the uncorrected, measured durations. Corrected mean open and burst durations were calculated by taking the

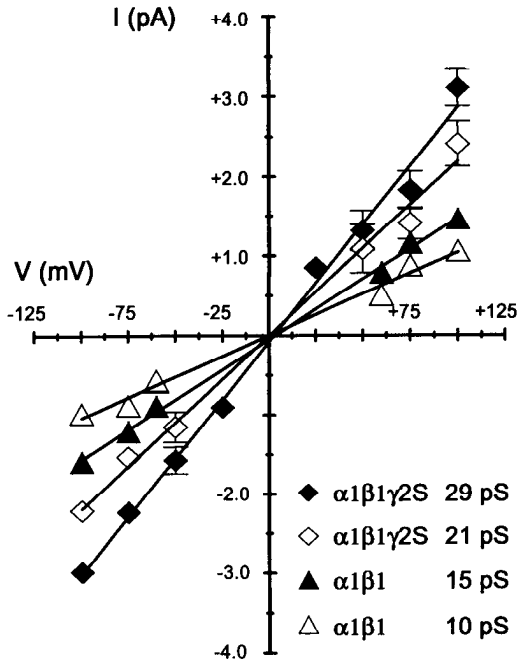

Figure 3. Current–voltage relationships for main conductance and subconductance levels of the $\alpha_1\beta_1$ and $\alpha_1\beta_1\gamma_{2S}$ GABARs. Single-channel amplitude histograms were constructed from openings recorded from excised outside-out patches containing either $\alpha_1\beta_1$ or $\alpha_1\beta_1\gamma_{2S}$ GABARs held at various holding potentials (−100 to +100 mV). The best Gaussian fits for both the main conductance and subconductance levels of each patch were determined at each holding potential. The average of the current amplitude means was calculated and plotted versus the holding potential for each receptor (*diamonds*, $\alpha_1\beta_1\gamma_{2S}$; *triangles*, $\alpha_1\beta_1$) and each level (*solid symbols*, main level; *open symbols*, subconductance level). Each point represents the average ± SEM for four to seven determinations. The signal-to-noise ratio was too low for reliable single-channel amplitude measurement when the holding potential approached ±25–50 mV (depending on the subunit combination). The best-fit line for the current–voltage relationship is shown. The calculated chord conductances for the $\alpha_1\beta_1$ GABAR channels were 10 and 15 pS, and for the $\alpha_1\beta_1\gamma_{2S}$ GABAR channels, 21 and 29 pS (subconductance and main conductance level, respectively).

sum of the relative area (a_i) of each exponential component in the respective duration histogram multiplied by the time constant (τ_i) of the component: corrected mean open/burst duration = $\Sigma\, a_i\tau_i$.

Amplitude histograms were constructed by binning channel openings (0.05 pA per bin width) that had a minimum duration of 0.5 msec ($\alpha_1\beta_1$) or 0.2 msec ($\alpha_1\beta_1\gamma_{2S}$) using the computer program IPROC (Axon Instruments, Burlingame, CA). These selection criteria were designed to measure true open channel amplitudes by eliminating from analysis all openings that were either baseline noise or too short in duration and thus had not reached true amplitude before closing. Histograms were fit with the sum of Gaussian curves to determine the mean amplitude of single-channel events.

Results

We have adopted the terminology initiated by Seeburg and colleagues for referring to recombinant GABARs produced upon the expression of multiple-subunit cDNAs (Draguhn et al., 1990; Verdoorn et al., 1990). For convenience, GABARs recorded from cells transfected with α_1 and β_1 or α_1, β_1, and γ_{2S} cDNAs were referred to as $\alpha_1\beta_1$ or $\alpha_1\beta_1\gamma_{2S}$ GABARs, respectively. This was not meant to imply that all GABAR channels recorded necessarily had the same subunit stoichiometry or configuration.

Single-channel conductance properties

Outside-out membrane patches were excised from L929 cells after transfection with either $\alpha_1\beta_1$ or $\alpha_1\beta_1\gamma_{2S}$ subunit cDNAs. At a holding potential of −75 mV, 3 μM GABA evoked a complex series of openings and closings in both receptor populations, as seen previously (Fig. 1). Single-channel currents from $\alpha_1\beta_1$ GABARs (Fig. 1, left) were composed of small-amplitude, brief duration openings that usually occurred as single events or brief bursts of openings and closings. In contrast, $\alpha_1\beta_1\gamma_{2S}$ GABARs (Fig. 1, right) produced single-channel openings that were longer in duration, were larger in conductance, and consisted more of prolonged bursts of openings. In neither case were openings seen in the absence of applied GABA. Approximately three-fourths of the patches from both cell populations contained GABARs (data not shown).

The amplitudes of single-channel openings from both receptor populations were measured by constructing amplitude histograms (Fig. 2*A*,*B*). A minimum open duration was chosen so that currents had reached their true maximum level (see Materials and Methods). Both $\alpha_1\beta_1$ and $\alpha_1\beta_1\gamma_{2S}$ GABARs opened

Table 1. Single-channel properties of $\alpha_1\beta_1$ and $\alpha_1\beta_1\gamma_{2S}$ GABARs

Property	$\alpha_1\beta_1$	$\alpha_1\beta_1\gamma_{2S}$
Chord conductance (pS)[a]		
Main level	15.3 ± 0.3	29.3 ± 0.7
Subconductance level	10.4 ± 0.5	21.3 ± 0.5
% Openings in Conductance Level[b]		
Main	88.8 ± 1.5 (n = 14)	66.4 ± 4.5 (n = 13)
Subconductance	11.2 ± 1.5 (n = 14)	33.6 ± 4.8 (n = 13)
% Current in Conductance Level[c]		
Main	99.2	89.4
Subconductance	0.9	10.6

Single-channel openings were elicited from excised outside-out membrane patches with various concentrations of applied GABA (1–10 μM). Values are the average ± SEM.

[a] The chord conductance was determined for the best-fit line shown in Figure 3. Values are significantly different among all levels within a given subunit combination and between the $\alpha_1\beta_1$ and $\alpha_1\beta_1\gamma_{2S}$ receptors ($p < 0.0001$, two-tailed t test).

[b] The percentage of openings in each conductance level was determined for each GABA application and averaged.

[c] The percentage of current in each conductance level was calculated from the total average current (Table 2).

Table 2. Recombinant GABAR main conductance and subconductance level open and closed properties

	$\alpha_1\beta_1$		$\alpha_1\beta_1\gamma_{2S}$	
	10 pS	15 pS	21 pS	29 pS
Opening/sec	0.86	9.2	4.0	9.7
Mean (corrected) open duration (msec)	0.39 (ND)	2.3 (2.1)	2.4 (2.4)	6.0 (5.6)
Mean percentage open	0.025	2.1	1.0	5.9
Total average current (fA)	0.23	25	15	126
Mean closed duration (msec)	1160	99.4	233	91.7
Number of openings	495	5320	3284	7963
Number of GABA applications	14	14	13	13

Openings per second, average (and corrected average) open duration, average current, percentage of analysis time open, average closed duration, and number of openings were determined from detected main conductance and subconductance level openings of $\alpha_1\beta_1$ and $\alpha_1\beta_1\gamma_{2S}$ GABARs evoked by 3 μM GABA (see Materials and Methods). ND, not determined.

to both a main conductance level and at least one subconductance level. Gaussian fits to each amplitude histogram (−75 mV) showed that $\alpha_1\beta_1$ GABARs had a main conductance level of 16.5 pS (1.24 pA) and a subconductance level of 12.0 pS (0.88 pA) as compared to $\alpha_1\beta_1\gamma_{2S}$ GABARs which had a main conductance level of 29.9 pS (2.24 pA) and a subconductance level of 19.5 pS (1.46 pA). Both conductance levels were apparent in single-channel traces (Fig. 1; *, subconductance level; **, main conductance level).

Single-channel current–voltage relationship

To determine more accurately the conductance levels of the two different GABAR populations, the chord conductances of $\alpha_1\beta_1$ and $\alpha_1\beta_1\gamma_{2S}$ GABARs were derived from single-channel current–voltage relationships. The means of the main conductance and subconductance levels calculated from several Gaussian-fitted amplitude histograms constructed at various holding potentials were plotted versus the holding potential (Fig. 3). Single-channel amplitudes were only calculated at holding potentials where both the main conductance and subconductance levels could be differentiated as two separate Gaussian peaks (i.e., ±60 to ±100 mV for $\alpha_1\beta_1$ GABARs). For both the main conductance and subconductance levels of $\alpha_1\beta_1$ and $\alpha_1\beta_1\gamma_{2S}$ GABARs, the current amplitude varied linearly with membrane holding potential and inverted at approximately 0 mV (E_{Cl} = 0 mV). The calculated chord conductances (Table 1) were 15.3 and 29.3 pS for the main conductance levels and 10.4 and 21.3 pS for the subconductance levels ($\alpha_1\beta_1$ and $\alpha_1\beta_1\gamma_{2S}$ GABARs, respectively). Main conductance level openings accounted for 88.8% (n = 14 applications) and 66.4% (n = 13 applications) of the openings of $\alpha_1\beta_1$ and $\alpha_1\beta_1\gamma_{2S}$ GABARs, respectively. The remaining 11.2% and 33.6% of openings were subconductance level openings. In terms of total current, 89.4% (126 fA) of the $\alpha_1\beta_1\gamma_{2S}$ GABAR current was through the main conductance level, with the remainder (10.6%, 15 fA) through the subconductance level (Table 2). Current through the $\alpha_1\beta_1$ GABAR main conductance level accounted for greater than 99% (25 fA) of the total average current as compared to the subconductance level current (0.23 fA). Thus, the GABARs formed by the expression of $\alpha_1\beta_1$ subunits can be differentiated from the GABARs formed from the expression of $\alpha_1\beta_1\gamma_{2S}$ subunits by a comparison of the resulting single-channel amplitudes.

Open and closed time properties

Analysis of GABAR single-channel currents evoked by 3 μM GABA revealed some similarities in gating properties of the main conductance and subconductance levels of $\alpha_1\beta_1$ and $\alpha_1\beta_1\gamma_{2S}$ GABARs (Table 2). For both receptor types, the main conductance level had a longer mean open duration than the subconductance level (2.3 vs 0.39 msec, $\alpha_1\beta_1$; 6.0 vs 2.4 msec, $\alpha_1\beta_1\gamma_{2S}$), which can also be seen in the raw data tracings (Fig. 1). Also, the ion channels opened more frequently to the main conductance level than to their corresponding subconductance level, and interestingly, the opening frequency for both $\alpha_1\beta_1$ and $\alpha_1\beta_1\gamma_{2S}$ GABAR main conductance levels were approximately 9–10 sec^{-1}. Since the mean percentage open during an application was dependent upon the mean open duration and opening frequency, this parameter was weighted in favor of the main conductance level for both ion channels. Thus, following transfection with all three subunits, GABARs were opened almost 6% of the time to the 29 pS level for the duration of the GABA application (as compared to 1.0% for the 21 pS level), and following transfection with only α_1 and β_1 subunit cDNAs, GABAR channels were opened 2.1% of the time to the 15 pS level (as compared to 0.025% for the 10 pS level). Corresponding mean closed durations were also similar between the main conductance and subconductance levels, with the main conductance levels for both ion channels ranging from 91 to 99 msec. Subconductance level openings had much longer mean closed durations ranging from 233 to 1160 msec, as would be predicted by their decreased opening frequency. The total average current through an excised membrane patch depended upon the single-channel amplitude, mean open duration, and opening frequency for a given opening. As would be predicted, $\alpha_1\beta_1$ GABAR subconductance level openings had the smallest amount of current (0.23 fA), followed by $\alpha_1\beta_1\gamma_{2S}$ GABAR subconductance level openings (15 fA), $\alpha_1\beta_1$ GABAR main conductance level openings (25 fA), and finally, $\alpha_1\beta_1\gamma_{2S}$ GABAR main conductance level openings (126 fA). The open and closed properties reported were derived from the combination of openings from all GABA applications; however, kinetic parameters were similar when compared on a per-application basis (data not shown).

Open duration frequency histograms for openings evoked by 3 μM GABA were prepared by pooling the open durations from all patches and applications (Fig. 4). $\alpha_1\beta_1$ GABAR subconductance level openings were not analyzed due to the low number of openings and their brief duration. As expected, 29 pS openings were shifted to longer-duration openings than 15 pS and 21 pS openings. The latter two open duration histograms were almost superimposable. The open duration frequency distributions were fitted best with sums of exponential functions. The $\alpha_1\beta_1$ GABAR 15 pS distribution was fitted best with the sum

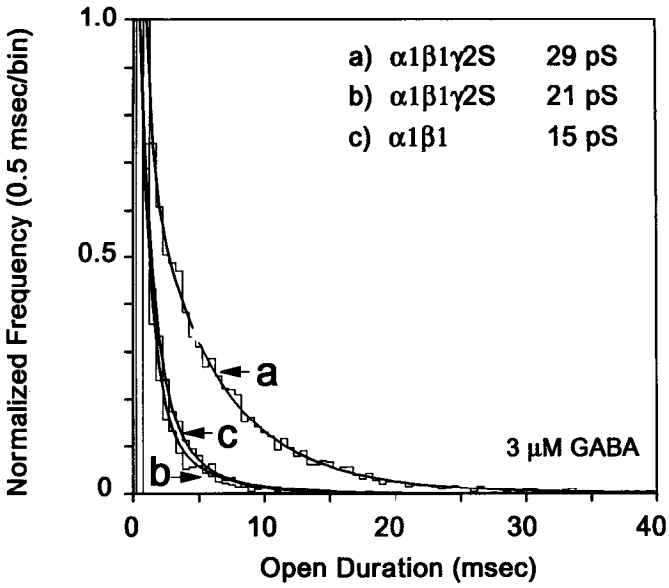

Figure 4. Open duration properties of $\alpha_1\beta_1$ and $\alpha_1\beta_1\gamma_{2S}$ recombinant GABARs. Open duration frequency histograms were obtained for single-channel openings of $\alpha_1\beta_1$ (main conductance level) and $\alpha_1\beta_1\gamma_{2S}$ (main conductance and subconductance levels) currents evoked with 3 μM GABA. Open durations were placed into 0.5 msec linear bins and displayed over a range of 1–40 msec. Open distributions were fitted best with the sum of two or three (see below) exponential functions and the calculated curves were superimposed over the histograms. Histograms and curves were normalized to area and superimposed. The *letters* and *arrows* denote the different subconductance and main conductance levels of $\alpha_1\beta_1$ and $\alpha_1\beta_1\gamma_{2S}$ GABARs.

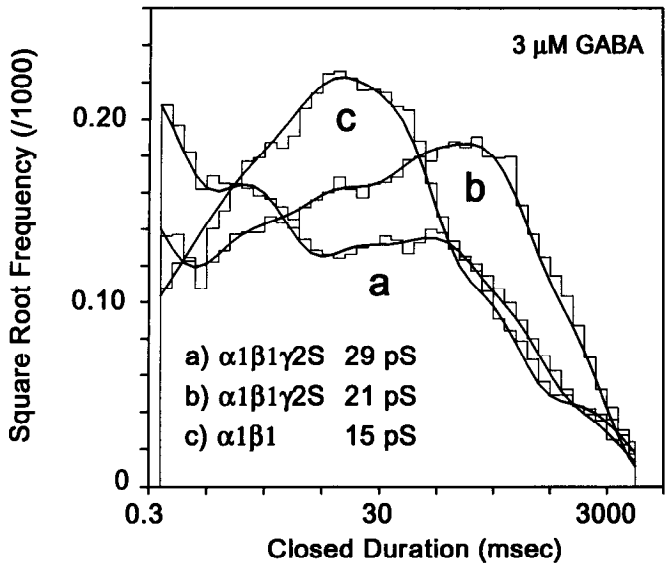

Figure 5. Closed duration properties of $\alpha_1\beta_1$ and $\alpha_1\beta_1\gamma_{2S}$ recombinant GABARs. Closed duration histograms for single-channel currents evoked by 3 μM GABA were constructed by placing closed durations into logarithmic bins (see Materials and Methods) and displayed over a range of 0.3 msec to 4.8 sec. Logarithmic histogram distributions were plotted as square-root transformed ordinate values (see Materials and Methods). Closed durations for $\alpha_1\beta_1$ GABAR main conductance level and $\alpha_1\beta_1\gamma_{2S}$ GABAR main conductance and subconductance levels were fitted best by the sum of five, six, and six exponential functions, respectively.

of two exponential functions, whereas both $\alpha_1\beta_1\gamma_{2S}$ GABAR distributions were fit with the sum of three exponential functions (Table 3). Exponential components were designated τ_1, τ_2, and τ_3 and corresponded to functions with the shortest to longest time constants, respectively. The first two time constants overlapped for all three receptor openings, ranging from 0.47 to 1.00 (τ_1) and from 3.2 to 4.4 msec (τ_2). The last time constant (τ_3) for $\alpha_1\beta_1\gamma_{2S}$ GABAR openings also overlapped and was approximately 8.0 msec. Even though the three different open duration frequency histograms were best described by overlapping exponential time constants, the corresponding curves differed due to the relative areas (a_i) for each time constant. The $\alpha_1\beta_1$ GABAR 15 pS open duration distribution was described by an equal weighting of the two shortest exponential time constants (τ_1 and τ_2), whereas the $\alpha_1\beta_1\gamma_{2S}$ GABAR 21 pS distribution was more heavily weighted to the shortest time constant, τ_1 (0.65 relative area), than the intermediate time constant, τ_2 (0.31 relative area). This distribution also had a small contribution by the longest time constant, τ_3 (0.04 relative area). The large shift in the $\alpha_1\beta_1\gamma_{2S}$ GABAR main conductance level open duration distribution to longer openings was due to the increased relative area of the two longer time constants (τ_2 and τ_3) and a decrease in the shortest time constant (τ_1).

Table 3. Recombinant GABAR open duration exponential components

	$\alpha_1\beta_1$, 15 pS	$\alpha_1\beta_1\gamma_{2S}$, 21 pS	$\alpha_1\beta_1\gamma_{2S}$, 29 pS
τ_1[a]	1.00 (0.93–1.1)	0.91 (0.85–0.99)	0.47 (0.29–0.85)
τ_2	3.2 (2.9–3.6)	4.4 (3.4–5.4)	4.2 (3.7–4.7)
τ_3	—	8.0 (Ind)	8.1 (7.3–8.9)
a_1[b]	0.48 (0.45–0.50)	0.65 (0.61–0.68)	0.09 (0.06–0.11)
a_2	0.52 (0.48–0.57)	0.31 (0.24–0.37)	0.47 (0.47–0.47)
a_3	—	0.04 (Ind)	0.44 (Ind)

Data are time constants (τ_i) and relative areas (a_i) for open and burst duration frequency histograms for the main conductance and subconductance levels of recombinant $\alpha_1\beta_1$ and $\alpha_1\beta_1\gamma_{2S}$ GABARs evoked by 3 μM GABA. The $\alpha_1\beta_1$ GABAR subconductance level openings were not analyzed (see Results). Histograms were fitted with the weighted sum of two or three exponential functions. The 95% confidence interval for all values are shown in parentheses. Ind, indeterminate.

[a] Data in msec.

[b] Normalized area.

The closed duration frequency histograms for $\alpha_1\beta_1$ main conductance level closures and $\alpha_1\beta_1\gamma_{2S}$ GABAR main conductance and subconductance level closures were obtained from pooled data of single-channel openings evoked by 3 μM GABA. The closed duration histograms were plotted using log binning with a square root transformation of the ordinate (Fig. 5) as described previously (Sigworth and Sine, 1987). Again, $\alpha_1\beta_1$ GABAR subconductance level closures were not analyzed due to the small number of closures. The distributions were fitted best with the sum of five ($\alpha_1\beta_1$ GABAR 15 pS level) or six ($\alpha_1\beta_1\gamma_{2S}$ GABAR 21 and 29 pS levels) exponential functions (Table 4). Time constants were designated τ_1–τ_6, from shortest to longest. The shortest time constant for the $\alpha_1\beta_1$ GABAR 15 pS level (1.1 msec) overlapped with the second-shortest time constant obtained for both levels of $\alpha_1\beta_1\gamma_{2S}$ GABAR channels; hence, it was designated τ_2, instead of τ_1, and the five time constants ranged from τ_2 to τ_6.

Again, the six time constants had overlapping ranges among the three different receptor/conductance levels. The longest closed duration time constants (τ_5 and τ_6) overlapped the least, but since their relative areas were small (see below), exact mea-

Table 4. Recombinant GABAR closed duration exponential components

	$\alpha_1\beta_1$, 15 pS	$\alpha_1\beta_1\gamma_{2S}$, 21 pS	$\alpha_1\beta_1\gamma_{2S}$, 29 pS
τ_1[a]	–	0.13 (0.10–0.16)	0.18 (0.16–0.20)
τ_2	1.1 (0.70–1.7)	1.2 (0.8–1.8)	1.5 (1.3–1.8)
τ_3	6.1 (5.0–7.5)	6.7 (5.1–8.8)	10.0 (7.7–13.2)
τ_4	25.9 (23.2–29.0)	33.8 (24.1–48.0)	56.9 (47.6–68.0)
τ_5	144 (121–171)	165 (143–191)	218 (188–251)
τ_6	1131 (853–1636)	635 (558–721)	979 (790–1242)
a_1[b]	–	0.23 (0.14–0.34)	0.42 (0.35–0.50)
a_2	0.11 (0.09–0.15)	0.09 (0.07–0.12)	0.24 (0.21–0.26)
a_3	0.28 (0.24–0.32)	0.15 (0.12–0.17)	0.10 (0.08–0.11)
a_4	0.45 (0.40–0.49)	0.14 (0.10–0.17)	0.13 (0.11–0.15)
a_5	0.13 (0.11–0.15)	0.28 (0.25–0.32)	0.10 (0.08–0.11)
a_6	0.02 (0.02–0.03)	0.11 (0.09–0.13)	0.02 (0.01–0.02)

Data are time constants (τ_i) and relative areas (a_i) for closed duration frequency histograms for the main conductance and subconductance levels of recombinant $\alpha_1\beta_1$ and $\alpha_1\beta_1\gamma_{2S}$ GABARs evoked by 3 μM GABA. The $\alpha_1\beta_1$ GABAR subconductance level closures were not analyzed (see Results). Histograms were fitted with the weighted sum of five or six exponential functions. The 95% confidence intervals for all values are shown in parentheses. Since the $\alpha_1\beta_1$ GABAR closed duration time constants correlated well with the five longest time constants determined for the $\alpha_1\beta_1\gamma_{2S}$ GABAR main conductance and subconductance levels, the first detected $\alpha_1\beta_1$ GABAR time constant (1.1 msec) was designated as τ_2. A corresponding shortest closed duration time constant (τ_1) for the $\alpha_1\beta_1$ GABAR main conductance level could not be fit.

[a] Data in msec.

[b] Normalized area.

surements could not be made with great accuracy. Thus, as was seen with the open duration time constants, all three receptor/conductance levels had similar closed duration time constants, and the shape of the distribution histogram was dictated by the relative areas of the time constants (Table 4). The $\alpha_1\beta_1\gamma_{2S}$ GABAR 29 pS closed duration distribution was dominated by the two shortest-duration time constants (τ_1 and τ_2), whereas the $\alpha_1\beta_1$ GABAR 15 pS and $\alpha_1\beta_1\gamma_{2S}$ GABAR 21 pS distributions were weighted more toward the intermediate (τ_3 and τ_4) and the longest (τ_5 and τ_6) time constants, respectively.

Burst properties

A burst was defined as a group of one or more openings separated by closures greater than a critical time, t_c (see Material and Methods). For this burst analysis, t_c was set at 5.0 msec. Bursts evoked by 3 μM GABA were compared for both the main conductance and subconductance levels of $\alpha_1\beta_1$ and $\alpha_1\beta_1\gamma_{2S}$ GABARs (Table 5). As would be predicted by the raw single-channel tracings (Fig. 1), $\alpha_1\beta_1\gamma_{2S}$ GABAR main conductance level bursts had the longest burst duration (17 msec), followed by $\alpha_1\beta_1$ GABAR main conductance level and $\alpha_1\beta_1\gamma_{2S}$ GABAR subconductance level bursts (both approximately 4.0 msec), and finally $\alpha_1\beta_1$ GABAR subconductance level bursts (0.41 msec). Although $\alpha_1\beta_1$ GABAR main conductance level bursts were more frequent (7.2 sec^{-1}) than the corresponding $\alpha_1\beta_1\gamma_{2S}$ GABAR bursts (4.1 sec^{-1}), their shorter duration caused the overall percentage of time in a burst (2.9%) to be less than that calculated for $\alpha_1\beta_1\gamma_{2S}$ GABAR bursts (6.9%). The number of openings per burst increased with single-channel amplitude, with $\alpha_1\beta_1$ GABAR subconductance bursts consisting of mostly single openings and $\alpha_1\beta_1\gamma_{2S}$ GABAR main conductance bursts averaging approximately three openings per burst. The mean percentage intraburst open time varied little among the three receptor/conductance levels. The burst properties obtained from the pooled data were similar to values obtained from individual applications (data not shown).

Table 5. Recombinant GABAR main conductance and subconductance level burst properties

	$\alpha_1\beta_1$		$\alpha_1\beta_1\gamma_{2S}$	
	10 pS	15 pS	21 pS	29 pS
Bursts/sec	1.0	7.2	3.1	4.1
Mean (corrected) burst duration (msec)	0.41 (ND)	4.0 (3.8)	3.8 (4.1)	17.0 (15.8)
Percentage of analysis time in burst	0.034	2.9	1.2	6.9
Mean percentage intraburst open time	ND	80.2	85.9	91.0
Mean number of openings/burst	1.0	1.4	1.4	2.6
Mean intraburst closed duration (msec)	ND	1.9	1.3	0.98
Mean interburst closed duration (msec)	ND	136	324	230
Number of bursts	487	3773	2336	3108
Number of GABA applications	14	14	13	13

Bursts per second, mean interburst closed time, mean burst duration, percentage of analysis time in burst, mean percentage intraburst open time, and number of bursts were derived from detected bursts and opening and closings within bursts evoked with 3 μM GABA from recombinant GABARS (see Materials and Methods). Percentage intraburst open time was calculated by taking the percentage of the total open time in a burst divided by the total time in a burst. Bursts were separated by closures of greater than 5 msec duration. ND, not determined.

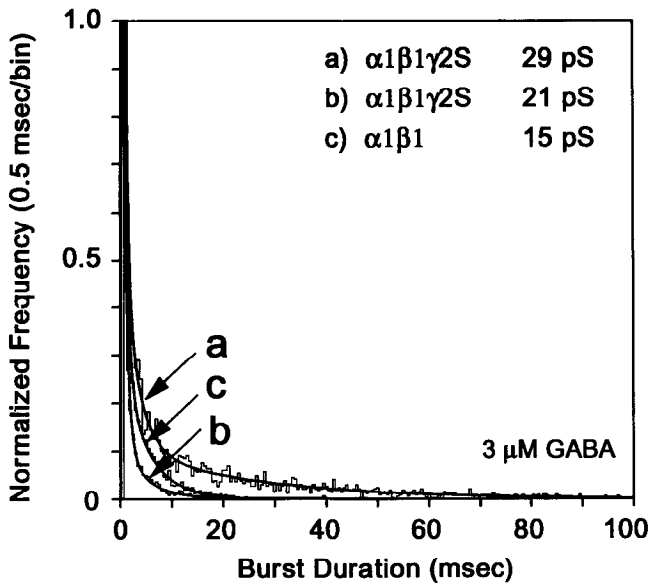

Figure 6. Burst duration properties of $\alpha_1\beta_1$ and $\alpha_1\beta_1\gamma_{2S}$ recombinant GABARs. Burst durations of single $\alpha_1\beta_1$ and $\alpha_1\beta_1\gamma_{2S}$ GABAR channels evoked with 3 μM GABA were placed into linear 0.5 msec bins and displayed over a range of 1–100 msec for clarity. The resulting frequency histograms were fitted best with either two ($\alpha_1\beta_1$) or three ($\alpha_1\beta_1\gamma_{2S}$) exponential functions that were superimposed on the distributions.

Burst duration distributions ranged from $\alpha_1\beta_1\gamma_{2S}$ GABAR main conductance level bursts, which were weighted to long bursts, to its corresponding subconductance bursts, which were predominantly short bursts (Fig. 6). $\alpha_1\beta_1$ GABAR main conductance level bursts were intermediate in their distribution. All three frequency histograms were also fitted best by the sum of two or three exponential functions. For each of the distributions, the three time constants, τ_1, τ_2, and τ_3, had overlapping values of approximately 0.70 msec, 4.0 msec, and 22 msec, respectively (Table 6). Again, $\alpha_1\beta_1$ GABAR main conductance level bursts were fitted best by the weighted sum of the two shortest time constants. As was seen for the open duration frequency histograms, the burst duration frequency histograms for $\alpha_1\beta_1\gamma_{2S}$ GABAR subconductance level bursts were heavily weighted to the shorter time constants, and this phenomenon was reversed for main conductance level bursts, which were predominantly composed of the longest-duration burst time constant.

Table 6. Recombinant GABAR burst duration exponential components

	$\alpha_1\beta_1$, 15 pS	$\alpha_1\beta_1\gamma_{2S}$, 21 pS	$\alpha_1\beta_1\gamma_{2S}$, 29 pS
τ_1[a]	0.80 (0.74–0.86)	0.68 (0.64–0.73)	0.56 (0.28–1.0)
τ_2	5.1 (4.7–5.5)	3.8 (3.1–4.7)	2.8 (1.8–4.3)
τ_3	—	19.1 (14.1–27.2)	25.4 (23.0–27.9)
a_1[b]	0.31 (0.29–0.32)	0.49 (0.46–0.52)	0.16 (0.10–0.21)
a_2	0.69 (0.65–0.74)	0.39 (0.33–0.45)	0.25 (0.18–0.32)
a_3	—	0.12 (0.09–0.16)	0.59 (0.51–0.68)

Data are time constants (τ_i) and relative areas (a_i) for open and burst duration frequency histograms for the main conductance and subconductance levels of recombinant $\alpha_1\beta_1$ and $\alpha_1\beta_1\gamma_{2S}$ GABARs evoked by 3 μM GABA. The $\alpha_1\beta_1$ GABAR subconductance level bursts were not analyzed (see Results). Histograms were fitted with the weighted sum of two or three exponential functions. The 95% confidence intervals for all values are shown in parentheses. [a] Data in msec.
[b] Normalized area.

Table 7. Comparison of 15 pS GABARs produced upon coexpression of $\alpha_1\beta_1$ and $\alpha_1\beta_1\gamma_{2S}$ subunits

	$\alpha_1\beta_1\gamma_{2S}$	$\alpha_1\beta_1$
Opening/sec	1.0	9.2
Mean open duration (msec)	1.5	2.3
Total average current (fA)	2	25
Mean closed duration (msec)	932	99.4
Bursts/sec	1.1	7.2
Mean burst duration (msec)	1.8	4.0
Mean number of openings/burst	1.1	1.4
Number of openings	863	5320
Number of bursts	798	3773
Number of GABA applications	13	14

Potential $\alpha_1\beta_1$ GABAR main conductance level openings and bursts produced in cells expressing α_1, β_1, and γ_{2S} subunits were detected after application of 3 μM GABA to membrane patches. Openings that fell within the 15 pS detection windows were analyzed with respect to their open, closed, and burst properties. For comparison, the values for the actual $\alpha_1\beta_1$ GABAR 15 pS main conductance level openings are listed from Tables 2 and 5.

$GABA_A$ receptor assembly

Since expression of $\alpha_1\gamma_{2S}$ and $\beta_1\gamma_{2S}$ subunits in a cell did not produce functional GABARs (Angelotti et al., 1993) and the ion channels produced upon the coexpression of $\alpha_1\beta_1$ and $\alpha_1\beta_1\gamma_{2S}$ subunits could be well differentiated by their single-channel amplitudes (Fig. 3) and open, closed, and burst properties (Tables 2, 5), it was possible to determine how prevalent $\alpha_1\beta_1$ GABARs were in a patch excised from a cell expressing $\alpha_1\beta_1\gamma_{2S}$ subunits. The lack of a 15 pS peak in the $\alpha_1\beta_1\gamma_{2S}$ GABAR amplitude histogram (Fig. 2*B*) suggested that they did not occur frequently. To perform a more complete examination, single-channel records of GABARs produced upon the coexpression of $\alpha_1\beta_1\gamma_{2S}$ subunits were analyzed for the presence of 15 pS "$\alpha_1\beta_1$-like" GABARs. The resulting open, closed, and burst properties of these GABARs were compared to those values obtained from authentic $\alpha_1\beta_1$ GABAR main conductance level openings (Table 7). Due to the differences in the open, closed, and burst properties, it seems most likely that the "$\alpha_1\beta_1$-like" GABAR openings represented incomplete openings to either the 21 or 29 pS level and not true $\alpha_1\beta_1$ 15 pS GABARs. Thus, it appeared that $\alpha_1\beta_1\gamma_{2S}$ GABARs were the final preferred form of the ion channel and that the formation of $\alpha_1\beta_1$ GABARs occurred predominantly in the absence of a coexpressed γ_{2S} subunit.

Discussion

Previously, we demonstrated that assembly of GABAR channels from α_1, β_1, and γ_{2S} subunits did not proceed randomly since not all combinations of subunits produce functional ion channels and GABARs formed after coexpression of $\alpha_1\beta_1\gamma_{2S}$ subunits produced a unique receptor expressing all three subunits (Angelotti et al., 1993). This article extends these findings by determining various single-channel properties of both $\alpha_1\beta_1$ and $\alpha_1\beta_1\gamma_{2S}$ GABARs, which allowed differentiation of the two receptor channel populations and confirmation that the latter form of the ion channel was preferred. In fact, in the presence of the γ_{2S} subunit, $\alpha_1\beta_1$ GABARs formed rarely, if at all. Analysis of the single-channel parameters of conductance amplitude and

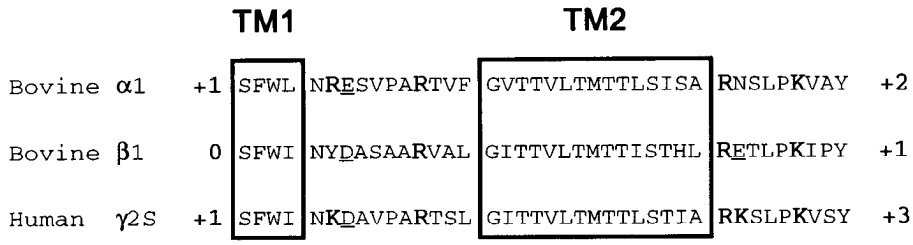

Figure 7. Amino acid alignment of the TM2 region of bovine α_1 and β_1 and human γ_{2S} GABAR subunits. Amino acid residues (single-letter code) of the TM2 region of the different GABAR subunits were shown with maximal alignment (Schofield et al., 1987; Pritchett et al., 1989). The last four amino acid residues of TM1 and the complete TM2 domain are *boxed.* The TM2 domain has been assigned according to the conserved exon/intron boundary determined by genomic cloning (Sommer et al., 1990; Kirkness et al., 1991). This assignment was more preferable since it placed a conserved ring of Arg (*R*) residues immediately proceeding the cytoplasmic side of TM2. Without this, the net charge on the cytoplasmic side of the β_1 subunit TM2 domain would be -1. The net charges on the cytoplasmic face of TM2 (*left*) and the extracellular face (*right*) for each subunit are listed. Positively charged residues are shown in *boldface,* and negatively charged residues are *underlined.*

open, closed, and burst properties also gave insight into other functional domains of the GABAR that may be conserved among subunits. These would include main conductance and subconductance levels, and the different open, closed, and burst states of the receptor.

$\alpha_1\beta_1$ and $\alpha_1\beta_1\gamma_{2S}$ GABARs had main conductance and subconductance level openings

Previously, it had been shown that GABARs composed of $\alpha_1\beta_1$ subunits had single-channel conductances of about 19 pS (Moss et al., 1990; Puia et al., 1990). The use of L929 cells for our expression studies created a higher signal-to-noise ratio that allowed for the observation of two conductance levels, a subconductance level of 10 pS and a main conductance level of 15 pS (Fig. 3). Coexpression of α_1 and β_1 subunits in HEK 293 cells (Verdoorn et al., 1990) produced GABARs with a 11 pS chord conductance. It was possible that substitution of the β_2 subunit for the β_1 subunit could have caused a decrease in the main conductance level, or it was possible that at the holding potential used for the amplitude histograms (-50 mV), the two Gaussian peaks could not be distinguished. Coexpression of $\alpha_1\beta_1\gamma_{2S}$ subunits produced GABARs that had a main and a subconductance level of 29 and 21 pS, respectively. The main conductance level was similar to that reported earlier for $\alpha_1\beta_2\gamma_{2S}$ GABARs expressed in HEK 293 cells, though no subconductance level was observed (Verdoorn et al., 1990). Thus, both $\alpha_1\beta_1$ and $\alpha_1\beta_1\gamma_{2S}$ GABARs had main conductance and subconductance levels, although the main conductance level accounted for 90% or greater of the total current through a patch for either GABAR. These results also proved that the subconductance level of $\alpha_1\beta_1\gamma_{2S}$ GABARs was not derived from openings of $\alpha_1\beta_1$ GABARs.

The conductance properties of nicotinic ACh receptors were shown to be due in a large part to the rings of negatively charged amino acids at the both ends of the ion channel pore (Imoto et al., 1988). These residues found immediately preceding and following the second transmembrane domain were thought to line the channel pore, and their negative charges may attract cations to pass through the ion channel. If the GABAR had a similar arrangement of subunit transmembrane domains, then an analogous ring of oppositely charged amino acids may be present (Stroud et al., 1990). Rings of positively charged amino acids, to attract chloride ions, would then be positioned in a similar manner. A comparison of the charges on the cytoplasmic and extracellular face of the bovine α_1, bovine β_1, and human γ_{2S} subunits suggested a reason for the increased single-channel conductance of the $\alpha_1\beta_1\gamma_{2S}$ GABARs (Fig. 7). The α_1 and γ_{2S} subunits possess a net charge of $+1$ on the cytoplasmic side, whereas the β_1 subunit has no net positive charge. On the extracellular side, the net positive charge increases from $+1$ (α_1), to $+2$ (α_1), to $+3$ (γ_{2S}). Thus, incorporation of a γ_{2S} subunit replacing either an α_1 or β_1 subunit(s) would cause a net increase in the positive charge at these important sites, with an exchange for β_1 leading to the greatest increase in charge. This would then most likely lead to an increase in the conductance of chloride ions through the channel. It is not known whether all of these positive charges are positioned in the lumen of the pore so as to affect conductance. If so, rectification of the single-channel currents might be expected due to the uneven distribution of positive charges on the cytoplasmic and extracellular surfaces of the channel. Mutational analysis of these charges and expression studies will be necessary to determine what amino acid residues are important in determining the conductance of GABARs.

$\alpha_1\beta_1$ and $\alpha_1\beta_1\gamma_{2S}$ GABARs possess dissimilar single-channel properties

A comparison of the open, closed, and burst properties of the different conductance levels of $\alpha_1\beta_1$ and $\alpha_1\beta_1\gamma_{2S}$ GABARs revealed some interesting trends. Open duration appeared to increase with increasing conductance level, from the 10 pS $\alpha_1\beta_1$ GABAR that had a very short open duration of less than 0.5 msec, to the 29 pS $\alpha_1\beta_1\gamma_{2S}$ GABAR with an average open time of 6.0 msec. The same trend was also found for the burst durations. Other trends cosegregate with either the main or the subconductance level of the $\alpha_1\beta_1$ and $\alpha_1\beta_1\gamma_{2S}$ GABARs. For example, both GABAR main conductance level openings had a larger opening frequency, larger total average current per patch, and larger mean percentage open time than the subconductance levels. In a similar fashion, both main conductance level bursts had a larger burst frequency, greater percentage of time in a burst, and more events per burst than the subconductance level bursts. As would be expected, the main conductance levels had shorter-duration closures and interburst closure times than found for the subconductance levels. Though the open, closed, and burst properties between $\alpha_1\beta_1$ and $\alpha_1\beta_1\gamma_{2S}$ GABAR main and conductance levels were different, the underlying gating properties were similar. All conductance level open and burst duration distribution histograms were fitted best with the weighted sum of two or three overlapping exponential functions, whereas the closed duration distribution histograms were fitted best with

five or six overlapping exponential functions. Single-channel analysis of both GABARs was performed with 3 μM GABA, and examination of the open, closed, and burst duration histograms (Figs. 4–6) revealed distinct differences in the subconductance and main conductance level openings. These results, coupled with the differences in chord conductances, suggested that the GABARs produced by coexpression of α_1 and β_1 or α_1, β_1, and γ_{2S} subunits were not identical. However, the similarity between $\alpha_1\beta_1$ and $\alpha_1\beta_1\gamma_{2S}$ GABAR main conductance level and subconductance level single-channel behaviors suggests that conserved amino acid residues among α_1, β_1, and γ_{2S} subunits probably account for the similar gating properties.

The absence of the longest open and burst duration time constant (τ_3) for $\alpha_1\beta_1$ GABAR main conductance level may have been due to the rarity of such long-duration openings or bursts. In a similar fashion, the absence of the shortest closed duration time constant (τ_1), which probably represented an intraburst closed time, may also have not been detected due to the opening and burst properties. Thus, the absence of such time constants may have been due to their low relative areas. This finding was not dependent upon the cell in which the subunits were expressed, since stable expression of $\alpha_1\beta_1$ GABARs in chinese hamster ovary cells also only produced two open and burst duration time constants (Porter et al., in press). Alternatively, the results may suggest that $\alpha_1\beta_1$ GABAR only opens and bursts from two open states instead of the three open states postulated for the mouse spinal cord neuron and $\alpha_1\beta_1\gamma_{2S}$ GABARs. Since $\alpha_1\beta_1\gamma_{2S}$ GABARs have a larger Hill coefficient than $\alpha_1\beta_1$ GABARs (1.7 vs 1.1, respectively) (Angelotti et al., 1993), the differences in the number of open, closed, and burst states detected in these two GABAR populations may reflect differences in the number of GABA binding sites. Further kinetic analysis is necessary to produce a kinetic gating model for the two GABAR channels that incorporates the different Hill coefficients.

Correlation of whole-cell currents with single-channel behavior

At maximal concentrations of GABA, whole-cell currents elicited from $\alpha_1\beta_1$ GABARs were one-fourth the magnitude of $\alpha_1\beta_1\gamma_{2S}$ GABAR currents (Angelotti et al., 1993), and this was due to the combination of several single-channel parameters. First, even though both $\alpha_1\beta_1$ and $\alpha_1\beta_1\gamma_{2S}$ GABARs had a main conductance and a subconductance level, approximately 90% of the current went through the main conductance level. The chord conductance of the $\alpha_1\beta_1\gamma_{2S}$ GABAR main conductance level was approximately twice that of $\alpha_1\beta_1$ GABARs (29 vs 15 pS, respectively), accounting for most of the difference between the whole-cell currents. Second, mean open and burst durations and frequencies were longer or larger for $\alpha_1\beta_1\gamma_{2S}$ GABARs, again causing a larger whole-cell current. Last, the exponential time constants that describe the open and burst duration histograms were similar, but their relative areas were shifted, with $\alpha_1\beta_1$ GABAR main conductance level openings being heavily weighted to short time constants and $\alpha_1\beta_1\gamma_{2S}$ GABAR main conductance level openings being heavily weighted toward longer time constants. The opposite was true for the closed duration histograms, where $\alpha_1\beta_1\gamma_{2S}$ GABARs were shifted to short closures, further increasing the percentage open time.

The single-channel kinetic parameters were determined for openings evoked with 3 μM GABA. At increasing concentrations of applied GABA (>3 μM), peak whole-cell currents obtained from $\alpha_1\beta_1\gamma_{2S}$ GABARs continued to increase whereas the concentration–response curve for $\alpha_1\beta_1$ GABARs began to plateau (Angelotti et al., 1993). This increase in the $\alpha_1\beta_1\gamma_{2S}$ GABAR whole-cell response was due to a concentration-dependent increase in the relative areas of the longest open and burst duration time constants, which was not found with $\alpha_1\beta_1$ GABARs (T. P. Angelotti, T. Ryan-Jastrow, and R. L. Macdonald, unpublished observations).

Comparison of recombinant and neuronal GABAR single-channel properties

Native GABARs from cultured fetal spinal cord and hippocampal neurons also exhibited a main conductance and subconductance level of approximately 27 and 19 pS (Hamill et al., 1983; Macdonald et al., 1989; Legendre and Westbrook, 1991). These values were similar to the two conductance levels recorded from $\alpha_1\beta_1\gamma_{2S}$ GABARs and suggested that the main conductance level of GABARs found in CNS neurons may result from an ion channel containing a γ subunit along with α and β subunits. Nonrectifying 15 pS GABA-gated ion channels have not been described as the main conductance level in cultured CNS neurons, suggesting that $\alpha_1\beta_1$ GABARs have not been observed (for review, see Mathers, 1991). Also, this combination of subunits probably did not constitute the adult guinea pig hippocampal GABAR reported by Gray and Johnston (1985), which was an outwardly rectifying GABA-gated channel of approximately 20 pS.

The similarity in the gating properties between the main conductance level of native GABARs and recombinant $\alpha_1\beta_1\gamma_{2S}$ GABARs further supports the hypothesis that a GABAR composed of α, β, and γ subunits may constitute the preferred form of the native GABAR. The derived time constants for open duration histograms, approximately 0.5, 4.0, and 8.0 msec, were similar to time constants obtained from open duration distributions describing GABAR ion channels from cultured mouse spinal cord neurons and rat hippocampal neurons (Macdonald et al., 1989; Legendre and Westbrook, 1991). In a similar fashion, the burst duration time constants and closed duration time constants were similar to time constants obtained for GABARs from mouse spinal cord neurons. These results together with the other whole-cell and single-channel properties demonstrated that the expression of recombinant GABARs can produce ion channels with pharmacological, conductance, and gating properties similar to native neuronal GABARs. For complete validation of recombinant GABARs as models of native receptors, development of a kinetic gating scheme for $\alpha_1\beta_1\gamma_{2S}$ GABARs will be necessary. For comparison to the mouse spinal cord neuron GABAR model, further analysis of single-channel openings at several different GABA concentrations will be required.

Assembly of a preferred configuration of $\alpha_1\beta_1\gamma_{2S}$ GABARs

Since expression of $\alpha_1\beta_1$ but not $\alpha_1\gamma_{2S}$ and $\beta_1\gamma_{2S}$ subunits in L929 cells produced functional ion channels, GABARs assembled after coexpression of α_1, β_1, and γ_{2S} subunits were easier to interpret than in previous studies where all combinations were observed (Verdoorn et al., 1990; Knoflach et al., 1992). Also, by studying expressed receptors with single-channel recording techniques, it was possible to obtain a "fingerprint" of their single-channel behavior, including conductance levels and open, closed, and burst properties. By combining all of these results, some general comments about the assembly of recombinant GABARs could be made.

Coexpression of α_1 β_1, and γ_{2S} subunits caused formation of

a unique ion channel that could be distinguished from the potential $\alpha_1\beta_1$ GABARs by its main conductance and subconductance levels. The virtual absence of any 10 or 15 pS $\alpha_1\beta_1$ GABARs (Fig. 2*B*) after coexpression of all three subunits suggested that the unique receptor channel formed from all three subunits was the preferred final form. Analysis of $\alpha_1\beta_1\gamma_{2S}$ GABAR single-channel current records with a 15 pS detection window did discern several potential "$\alpha_1\beta_1$-like" GABAR openings, but a comparison of the kinetic properties of $\alpha_1\beta_1$ and the few $\alpha_1\beta_1\gamma_{2S}$ GABAR 15 pS single-channel currents revealed distinct differences. A complete comparison of the mean open, closed, and burst duration, mean total average current, and mean number of openings/burst between the two 15 pS GABARs indicated that $\alpha_1\beta_1\gamma_{2S}$ GABAR single-channel currents probably represented short-duration, single opening bursts that had not reached their maximum amplitude and were not true $\alpha_1\beta_1$ GABAR single-channel openings. This result implied that the unique GABAR formed upon coexpression of the α_1 β_1, and γ_{2S} subunits within the same cell was a preferred form of the ion channel relative to $\alpha_1\beta_1$ GABARs. This finding was consistent with the conclusion reached by others using whole-cell electrophysiological properties such as desensitization kinetics and Zn^{2+} inhibition (Draguhn et al., 1990; Verdoorn et al., 1990). The unique conductance properties of the two different receptor populations suggested that the subconductance state of the preferred form of the ion channel was not due to the appearance of other, less preferred forms, as suggested for mouse nicotinic ACh receptors (Kullberg et al., 1990).

It was calculated that 51 different configurations of a GABAR with three subunits (α_1, β_1, and γ_{2S}) were possible, assuming a pentameric arrangement (Burt and Kamatchi, 1991). A configuration may have the same stoichiometry of subunits, but in different pentameric arrangements. Of these, 3 were single-subunit configurations, which probably did not assemble in L929 cells, 18 were two-subunit configurations (six per pair of subunits), and the remaining 30 contained all three subunits. Of the 18 two subunit configurations, 12 were potentially $\alpha_1\gamma_{2S}$ and $\beta_1\gamma_{2S}$ GABAR configurations; hence, these were also not found in this cell expression system. Thus, 36 different GABAR configurations could exist. The appearance of a main conductance and a subconductance level for both $\alpha_1\beta_1$ and $\alpha_1\beta_1\gamma_{2S}$ GABARs may arise from two separate configurations of either subunit combination or two transition states of the same receptor configuration. If there existed two separate configurations, then the main conductance state was a more preferred form since it accounted for at least two-thirds of the openings and 90% of the current. The exact nature of the subconductance state of a GABAR is not known, but recent work has suggested that the subconductance level is a transition from the main conductance level. The conclusion was made based upon the finding that the subconductance openings were more commonly found preceding or succeeding a main conductance opening, suggesting that the two openings were linked and not independent openings of two distinct ion channels (Twyman and Macdonald, 1992). Also, direct transitions between conductance levels have been observed after the expression of other α and β subunits (data not shown).

Theoretically, it was possible that all six of the $\alpha_1\beta_1$ GABAR configurations and 30 of the $\alpha_1\beta_1\gamma_{2S}$ GABAR configurations could exist and that they all had the same conductance properties, open, closed, and burst properties, and exponential time constants. Incorporation of the γ_{2S} subunit in the final GABAR increased the main conductance level from 15 to 29 pS, much the same way that incorporation of the δ subunit of the nicotinic ACh receptor with α, β, and γ subunits increased the conductance from 12 to 50 pS (Kullberg et al., 1990). If the γ_2 subunit was assembled with other α_1 and β_1 subunits at random stoichiometries, then other ion channels with discrete, incremental conductances would be formed and seen as complex amplitude histograms. Such a hypothesis was tested with the analysis of neuronal nicotinic receptors, to determine the stoichiometry of the non-α and β subunits (Cooper et al., 1991). The lack of such complex amplitude histograms suggested that the stoichiometry of recombinant GABAR composed of $\alpha_1\beta_1\gamma_{2S}$ subunits was fixed, though either four or six pentameric configurations may exist for a given ratio of three subunits.

Most $\alpha_1\beta_1\gamma_{2S}$ GABAR patches analyzed had nonmultiple openings, suggesting that the patches contained one or possibly two ion channels (data not shown). A patch-by-patch analysis of the single-channel properties of $\alpha_1\beta_1\gamma_{2S}$ GABARs revealed that the open, closed, and burst properties did not vary from those derived from the entire data set combined (data not shown). Thus, it appeared that the ion channel openings present in different cells and membrane patches following different transfections were derived from GABARs with similar properties. It was possible that all four or six potential configurations would produce equivalent single-channel "fingerprints," but this seemed less likely considering the similar, but distinct, properties of GABAR composed of only $\alpha_1\beta_1$ subunits.

The assembly path that eventually led to the production of $\alpha_1\beta_1\gamma_{2S}$ GABARs is not known yet. Considering the homology among the functional domains of the various subunits of the nicotinic ACh receptor supergene family, it is likely that $\alpha_1\beta_1$ GABARs may form from intermediates of the assembly path, similar to the formation of $\alpha\gamma$ and $\alpha\delta$ dimers of nicotinic ACh receptors (Blount et al., 1990; Gu et al., 1991). The demonstration that there existed a final preferred configuration of the $\alpha_1\beta_1\gamma_{2S}$ GABAR must ultimately be confirmed using biochemical or immunocytochemical techniques. Using the high resolution of single-channel recording, it was possible to demonstrate that GABAR subunits can assemble in a nonrandom fashion to produce receptors with similar gating properties. By repeating these experiments with recombinant GABARs composed of other combinations of α, β, and γ isoforms and other subunits, it should be possible to produce single-channel "fingerprints" for comparison to native GABARs. By combining this information with the expression patterns of receptor subunit mRNAs (Laurie et al., 1992; Wisden et al., 1992), it may be possible to determine the exact GABARs expressed in various brain regions and to determine the underlying architecture of inhibitory synaptic transmission.

References

Angelotti TP, Uhler MD, Macdonald RL (1993) Assembly of $GABA_A$ receptor subunits: analysis of transient single-cell expression utilizing a fluorescent substrate/marker gene technique. J Neurosci 13:1418–1428.

Blair LA, Levitan ES, Marshall J, Dionne VE, Barnard EA (1988) Single subunits of the $GABA_A$ receptor form ion channels with properties of the native receptor. Science 242:577–579.

Blount P, Smith MM, Merlie JP (1990) Assembly intermediates of the mouse muscle nicotinic acetylcholine receptor in stably transfected fibroblasts. J Cell Biol 111:2601–2611.

Burt DR, Kamatchi GL (1991) $GABA_A$ receptor subtypes—from pharmacology to molecular biology. FASEB J 5:2916–2923.

Chen C, Okayama H (1987) High-efficiency transformation of mammalian cells by plasmid DNA. Mol Cell Biol 7:2745–2752.

Colquhoun D, Sigworth FJ (1983) Fitting and statistical analysis of single-channel records. In: Single channel recordings (Sakmann B, Neher E, eds), pp 191–263. New York: Plenum.

Cooper E, Couturier S, Ballivet M (1991) Pentameric structure and subunit stoichiometry of a neuronal nicotinic acetylcholine receptor. Nature 350:235–238.

Draguhn A, Verdoorn TA, Ewert M, Seeburg PH, Sakmann B (1990) Functional and molecular distinction between recombinant rat $GABA_A$ receptor subtypes by Zn^{2+}. Neuron 5:781–788.

Gray R, Johnston D (1985) Rectification of single GABA-gated chloride channels in adult hippocampal neurons. J Neurophysiol 54:134–142.

Gu Y, Forsayeth JR, Verrall S, Yu XM, Hall ZW (1991) Assembly of the mammalian muscle acetylcholine receptor in transfected COS cells. J Cell Biol 114:799–807.

Hamill OP, Bormann J, Sakmann B (1983) Activation of multiple-conductance state chloride channels in spinal neurones by glycine and GABA. Nature 305:805–808.

Imoto K, Busch C, Sakmann B, Mishina M, Konno T, Nakai J, Bujo H, Mori Y, Fukuda K, Numa S (1988) Rings of negatively charged amino acids determine the acetylcholine receptor channel conductance. Nature 335:645–648.

Kirkness EF, Kusiak JW, Fleming JT, Menninger J, Gocayne JD, Ward DC, Venter JC (1991) Isolation, characterization, and localization of human genomic DNA encoding the beta 1 subunit of the $GABA_A$ receptor (GABRB1). Genomics 10:985–995.

Knoflach F, Backus KH, Giller T, Malherbe P, Pflimlin P, Mohler H, Trube G (1992) Pharmacological and electrophysiological properties of recombinant $GABA_A$-receptors comprising the $alpha_3$-subunit, $beta_1$-subunit and $gamma_2$-subunit. Eur J Neurosci 4:1–9.

Kullberg R, Owens JL, Camacho P, Mandel G, Brehm P (1990) Multiple conductance classes of mouse nicotinic acetylcholine receptors expressed in *Xenopus* oocytes. Proc Natl Acad Sci USA 87:2067–2071.

Laurie DJ, Seeburg PH, Wisden W (1992) The distribution of 13 $GABA_A$ receptor subunit messenger RNAs in the rat brain. II. Olfactory bulb and cerebellum. J Neurosci 12:1063–1076.

Legendre P, Westbrook GL (1991) Noncompetitive inhibition of gamma-aminobutyric $acid_A$ channels by Zn. Mol Pharmacol 39:267–274.

Levitan ES, Blair LAC, Dionne VE, Barnard EA (1988) Biophysical and pharmacological properties of cloned $GABA_A$ receptor subunits expressed in *Xenopus* oocytes. Neuron 1:773–781.

Macdonald RL, Rogers CJ, Twyman RE (1989) Kinetic properties of the $GABA_A$ receptor main conductance state of mouse spinal cord neurones in culture. J Physiol (Lond) 410:479–499.

Mathers DA (1991) Activation and inactivation of the $GABA_A$ receptor—insights from comparison of native and recombinant subunit assemblies. Can J Physiol Pharmacol 69:1057–1063.

McManus OB, Blatz AL, Magleby KL (1987) Sample, log binning, fitting and plotting durations of open and shut intervals from single channels and the effects of noise. Pfluegers Arch Eur J Physiol 410: 530–553.

Moss SJ, Smart TG, Porter NM, Nayeem N, Devine J, Stephenson FA, Macdonald RL, Barnard EA (1990) Cloned GABA receptors are maintained in a stable cell line: allosteric and channel properties. Eur J Pharmacol [Mol Pharmacol] 189:77–88.

Olsen RW, Tobin AJ (1990) Molecular biology of $GABA_A$ receptors. FASEB J 4:1469–1480.

Paulson HL, Ross AF, Green WN, Claudio T (1991) Analysis of early events in acetylcholine receptor assembly. J Cell Biol 113:1371–1384.

Porter NM, Twyman RE, Uhler MD, Macdonald RL (1990) Cyclic AMP-dependent protein kinase decreases $GABA_A$ receptor current in mouse spinal neurons. Neuron 5:789–796.

Porter NM, Angelotti TP, Twyman RE, Macdonald RL (in press) Kinetic properties of $\alpha 1\beta 1$ $GABA_A$ receptor channels expressed in CHO cells: regulation by pentabarbitone and picrotoxin. Mol Pharmacol, in press.

Pritchett DB, Sontheimer H, Shivers BD, Ymer S, Kettenmann H, Schofield PR, Seeburg PH (1989) Importance of a novel $GABA_A$ receptor subunit for benzodiazepine pharmacology. Nature 338:582–585.

Puia G, Santi MR, Vicini S, Pritchett DB, Purdy RH, Paul SM, Seeburg PH, Costa E (1990) Neurosteroids act on recombinant human $GABA_A$ receptors. Neuron 4:759–765.

Saedi MS, Conroy WG, Lindstrom J (1991) Assembly of *Torpedo* acetylcholine receptors in *Xenopus* oocytes. J Cell Biol 112:1007–1015.

Schofield PR, Darlison MG, Fujita N, Burt DR, Stephenson FA, Rodriguez H, Rhee LM, Ramachandran J, Reale V, Glencorse TA, Seeburg PH, Barnard EA (1987) Sequence and functional expression of the $GABA_A$ receptor shows a ligand-gated receptor superfamily. Nature 328:221–227.

Shivers BD, Killisch I, Sprengel R, Sontheimer H, Kohler M, Schofield PR, Seeburg PH (1989) Two novel $GABA_A$ receptor subunits exist in distinct neuronal subpopulations. Neuron 3:327–337.

Sigel E, Baur R, Trube G, Mohler H, Malherbe P (1990) The effect of subunit composition of rat brain $GABA_A$ receptors on channel function. Neuron 5:703–711.

Sigworth FJ, Sine SM (1987) Data transformations for improved display and fitting of single-channel dwell time histograms. Biophys J 52:1047–1054.

Smart TG, Moss SJ, Xie X, Huganir RL (1991) $GABA_A$ receptors are differentially sensitive to zinc—dependence on subunit comparison. Br J Pharmacol 103:1837–1839.

Sommer B, Poustka A, Spurr NK, Seeburg PH (1990) The murine $GABA_A$ receptor delta-subunit gene—structure and assignment to human chromosome-1. DNA Cell Biol 9:561–568.

Stroud RM, McCarthy MP, Shuster M (1990) Nicotinic acetylcholine receptor superfamily of ligand-gated ion channels. Biochemistry 29: 11009–11023.

Sumikawa K, Gehle VM (1992) Assembly of mutant subunits of the nicotinic acetylcholine receptor lacking the conserved disulfide loop structure. J Biol Chem 267:6286–6290.

Toyoshima C, Unwin N (1990) Three-dimensional structure of the acetylcholine receptor by cryoelectron microscopy and helical image reconstruction. J Cell Biol 111:2623–2635.

Twyman RE, Macdonald RL (1992) Neurosteroid regulation of $GABA_A$ receptor single-channel properties of mouse spinal cord neurons in culture. J Physiol (Lond) 456:215–245.

Verdoorn TA, Draguhn A, Ymer S, Seeburg PH, Sakmann B (1990) Functional properties of recombinant rat $GABA_A$ receptors depend upon subunit composition. Neuron 4:919–928.

Wisden W, Laurie DJ, Monyer H, Seeburg PH (1992) The distribution of 13 $GABA_A$ receptor subunit messenger RNAs in the rat brain. I. Telencephalon, diencephalon, mesencephalon. J Neurosci 12:1040–1062.